Radiation Spectroscopy of Gamma-Rays

工物 22 杨哲涵 2022011105

My reference is the book Radiation detection and measurement, 4th ed by Glenn F. Knoll. And in this arctile I will follow the structure of Chapter 10 in the book and discuss the critical mechanisms of gamma-ray spectroscopy with scintillators.

1. Introduction

X-ray or gamma-ray photons are uncharged and therefore primarily invisible to the detector. The key of detecting them is to first convert incident photons into fast electrons and then collect these electrons.

Since the stopping power of gases is low, e.g. 1 MeV electron in STP gases can penetrate for several meters and most gamma-ray incuded pulses from a gas-filled counter actually arise from the solid counter wall and have lost varialbe energy in the wall, gas-filled detectors are not suitable for gamma-ray spectroscopy.

The thallium-activated sodium iodine scintillation detector arose in the 1950s have proven the effectiveness of scintillation detectors in gamma-ray spectroscopy.

2. Review on Gamma-Ray Interactions

In Chapter 2 we have studied the three interaction mechnisms of significance in gamma-ray spectroscopy. The dominant parameters in these three interactions are $h\nu$, the photon’ s energy and Z, the atomic number of the absorbing material.

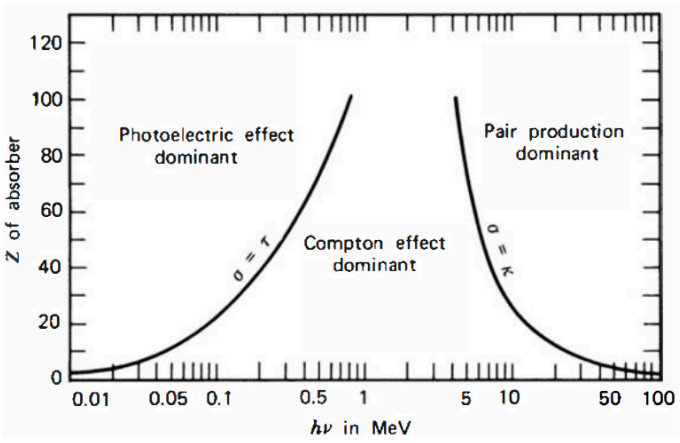

Figure 1: Relative importance of three main gamma-ray interactions

2.1. Photoelectric Absorption

Photoelectric absorption is an interaction that absorbs the photon and emits a photoelectron of the energy:

$$E_{e^-} = h\nu - E_b \tag{1}$$

Where E_b is the binding energy and is in the form of a characteristic X-ray or Auger electron[1]. Most possibly, photoelectron emerges from the K shell, whose typcial binding energy ranges from few keV ($_{11}$Na, 1keV) to hundred keV($_{88}$Ra, 100keV).

2.2. Compton Sacttering

The result of Compton scattering is a scattered photon and a recoil electron.

$$\begin{aligned} h\nu' &= \frac{h\nu}{(1+(h\nu)/m_0c^2)(1-\cos\theta)} \\ E_{e^-} &= h\nu - h\nu' \end{aligned} \tag{2}$$

The angular distribution of scattered gamma rays is predicted by the Klein-Nishina formula and is ploted polarly in Figure 2.

$$\begin{aligned} \frac{\mathrm{d}\sigma}{\mathrm{d}\Omega} &= Zr_0^2\left(\frac{1}{1+\alpha(1-\cos\theta)}\right)^2\left(\frac{1+\cos^2\theta}{2}\right) \\ &\left(1+\frac{\alpha^2(1-\cos\theta^2)}{(1+\cos^2\theta)(1+\alpha(1-\cos\theta))}\right) \\ \alpha &= h\nu/m_0c^2, r_0 = \text{classical electron radius} \end{aligned} \tag{3}$$

[1] Auger electrons have extremly short range because of their low energy

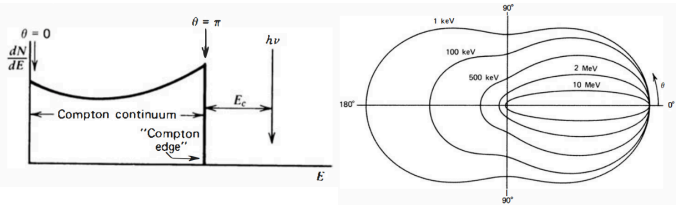

Compton edge Klein-Nishina formula

Figure 2: Compton sacttering

And generally the shape of the electron energy distribution has a so-called Compton edge.

2.3. Pair Production

The process occurs in the intense electric field near the protons in the nuclei of the absorbing material and corresponds to the creation of an electron-positron pair at the point of complete disappearance of the incident gamma-ray photon.

$$E_{e^-} + E_{e^+} = h\nu - 2m_0c^2 \tag{4}$$

Once the kinetic energy of the positron is lost, it will annihilate with or combine with a normal electron in the absorbing medium, which will make the spectroscopy analysis more complicated as we shall see later.

3. Predicted Response Function

We have discussed the three main mechanisms of gamma-ray interactions. Their simplest energy spectrum of their own is presented in Figure 3.

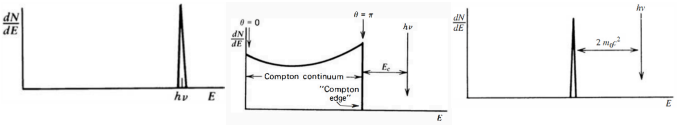

Figure 3: Three main mechanisms in gamma-ray interactions

3.1. Ideal Case of Intermediate Detectors

As for practical detectors, the actual response is much more complicated. All these interactions take place and the properties of the detector material and the geometry of the detector will affect the response function as well as the cirumstances.

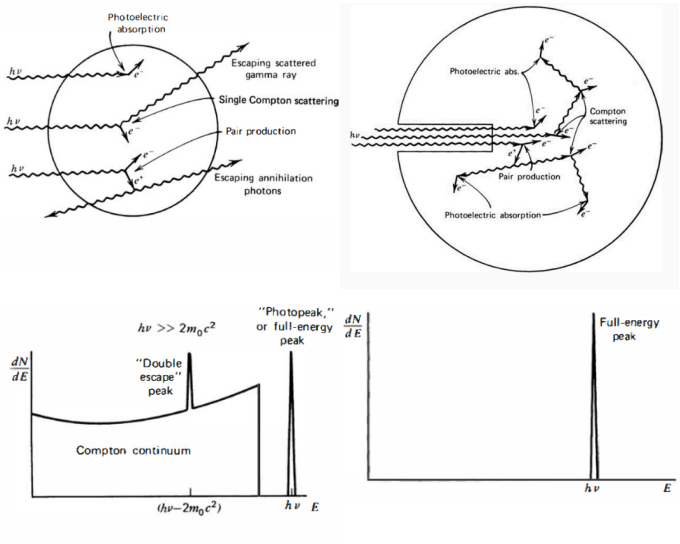

Figure 4: Small detector VS extreme large detector

As stated in Figure 4, the spectrum depends on whether all primary and Secondary interactions happen within the active volume of the detector or not.

The real detectors are all of medium size and we can never achieve the ideal case of all interactions happening within the active volume since there are always interactions near the entrance surface.

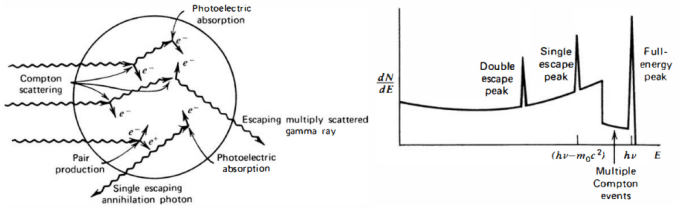

Figure 5: Real detector

It’s worth mentioning that there is “Multiple Compton events”. The multiple Compton events arise from the escape of the final scattered photons, which can thus partially fill in the gap between the Compton edge and the photopeak.

3.2. Complications in the Real Response

There are several more complicated cases than those shown in Figure 5.

3.2.1. Secondary Electron Escape

Especially for high energy gamma-rays, the Secondary electrons may escape the active volume since their range is larger than the size of the detector. This effect will alter the shape of the Compton continuum and lower the

photofraction due to envents loss from the photopeak.

3.2.2. Bremsstrahlung Escape

Radiative processes for charged particles due to coulomb interactions are Bremsstrahlung, where energy converts into electromagnetic radiation. The linear specific energy loss is:

$$-\left(\frac{\mathrm{d}E}{\mathrm{d}x}\right)_r = \frac{NEZ(Z+1)e^4}{137m_0^2c^4}\left(4\ln\frac{2E}{m_0c^2} - \frac{4}{3}\right) \quad (5)$$

Again for high energy (few MeV and above) gamma-rays and high atomic number absorber case, the Bremsstrahlung loss is of importance.

3.2.3. Characteristic X-ray Escape

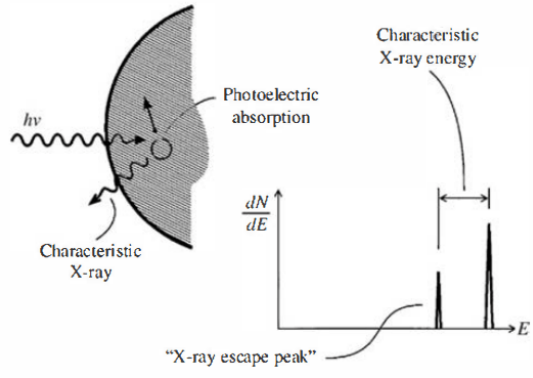

Figure 6: X-ray escape mechanism

Normally characteristic X-ray emission is reabsorbed near where it is produced. But if the photoelectric absorption occurs near a surface of the detector, the X-ray may escape and so does its energy. This gives rise to a new peak below the full energy photopeak. Usually we can only distinguish the K-shell X-ray escape peak from the photopeak.

3.2.4. Secondary Radiations Created Near the Source

3.2.4.1. Annihilation Peak

If the gamma-ray source happens to emit positrons, a peak of 0.511 MeV will rise since the positron will annihilate when stopped in the surrounding covering. Sometimes if the detector can detect both annihliation photons simutaneously, a peak of 1.022 MeV will appear.

3.2.4.2. Bremsstrahlung

Most commonly available gamma-ray sources are β^- emitters at the same time. And Bremsstrahlung photons (low energy most possibly) will contribute to the spectrum due to absorption of β^- decays in the encapsulation. So use of low atomic number absorbers will help minimize the generationn of Bremsstrahlung.

3.2.5. Effects of Surrounding Materials

3.2.5.1. Backscatterd Gamma-Rays

As discussed before, the energy of backscattered photon is:

$$h\nu'|_{\theta=\pi} = \frac{h\nu}{1+2h\nu/m_0c^2} \quad (6)$$

And in the limit of $h\nu \gg m_0c^2$, the energy reduces to $m_0c^2/2$. The backscatter peak always occurs at 0.255 MeV or less.

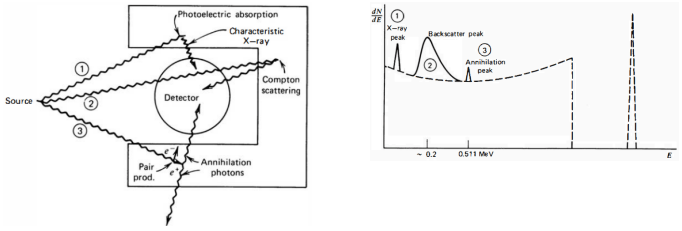

Figure 7: Backscatterd gamma-rays

3.2.5.2. Other Secondary Radiations

Other interaction of the primary gamma-rays in the surrounding materials, for example, characteristic X-rays, will reach the detector and produce noticeable peaks. One method to reduce the effect is to use graded shields consisting of high-Z bulk and low-Z inner layers. The inner layers will absorb the strong characteristic X-rays from the bulk and only emit weak X-rays on their own.

Another effect of high energy primary gamma-rays is the enhanced pair production process within high-Z surrounding materials.

3.2.6. Coincidence Methods in Gamma-Ray Spectrometers

To achieve ideal delta response function, some steps are taken at the price of added complexity. For the case of sodium iodide spectrometers, the most common methods involve the use of an annular detector surrounding the primary crystal for Compton suppression by anticoincidence.

And here is an example from germanium detectors in Figure 8, coincidence detection of

the escaping photons in a surrounding annular detector(BGO and NaI(Tl)[2])

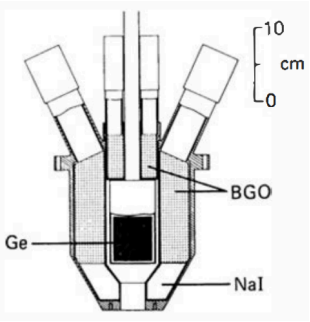

BGO and NaI(Tl) scintillators combined Compton suppression system

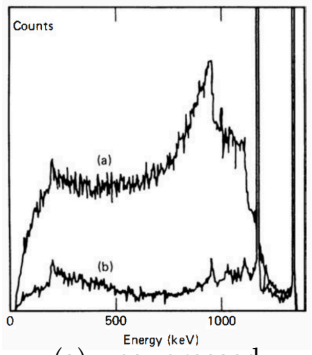

(a):unsupressed

(b): suppressed

Figure 8: Anticoincidence Compton Suppression

4. Properties of Scintillation Gamma-Ray Spectrometer

4.1. Response Function

Sodium iodide (NaI) gained popularity due to the high atomic number ($Z = 53$) of its iodine component, which enhances photoelectric absorption, resulting in high intrinsic detection efficiency and a large photofraction. This combination has led to the success of NaI scintillation spectrometers. Despite newer scintillators like LaBr3(Ce) offering higher light yield and better energy resolution, NaI(Tl) remains widely used due to its balance of low cost, availability, and adequate performance. Detailed studies and extensive experimental data on NaI(Tl) have further solidified its reliability and predictability in gamma-ray spectroscopy. NaI(Tl) also shows significantly better energy resolution compared to materials like BGO (see to Figure 9).

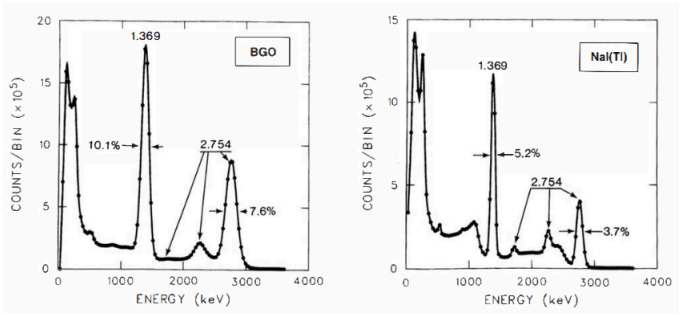

Figure 9: Comparative pulse height spectra measured for BGO and NaI

Due to the challenges in experimentally measuring the gamma-ray response function across all energies, calculations using the Monte Carlo method (see Figure 10) are essential, as they effectively model complex interactions within detectors. Additionally, for organic scintillators, which have low photoelectric interaction probabilities, deconvolution techniques can enhance gamma-ray spectra analysis (see Figure 10). These methodologies underscore the critical role of advanced computational and analytical techniques in gamma-ray spectroscopy.

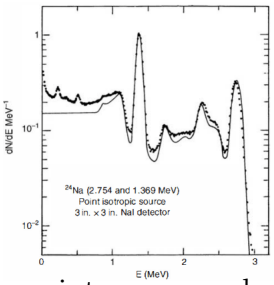

points: measured

line: Monte Carlo

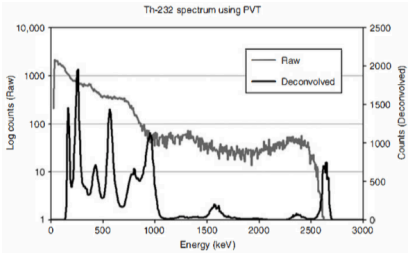

example of the application of deconvolution methods

Figure 10: Anticoincidence Compton Suppression

4.2. Energy Resolution

The energy resolution R is defined as

$$R = \frac{\text{FWHM}}{H_0}$$

$$\text{where } H_0 = \text{mean pulse height} \tag{7}$$

As argued in Chapter 4, the finite energy resolution of any detector may contain contributions resulting from the effects of charge collection statistics, electronic noise, variations in the detector response over its active volume, and drifts in operating parameters over the course of the measurement.

[2]BGO has the strong advantage that its high density and atomic number allow a more compact configuration compared with a sodium iodide detector of the same detection efficiency.

Howerver, the charge collection statistics, i.e. photoelectron statistics is the dominant factor in the energy resolution of scintillation detectors.

Therefore

$$R = \frac{\text{FWHM}}{H_0} = K\frac{\sqrt{E}}{E} \propto \frac{1}{\sqrt{E}} \tag{8}$$

If we take logarithm of both sides, we derive

$$\ln R = \ln K - \frac{1}{2}\ln E \tag{9}$$

And a more adequate representation of measured data takes the form

$$R = \frac{\sqrt{\alpha + \beta E}}{E} \tag{10}$$

where α, β are constants particular to any specific scintillator-PMT combination.

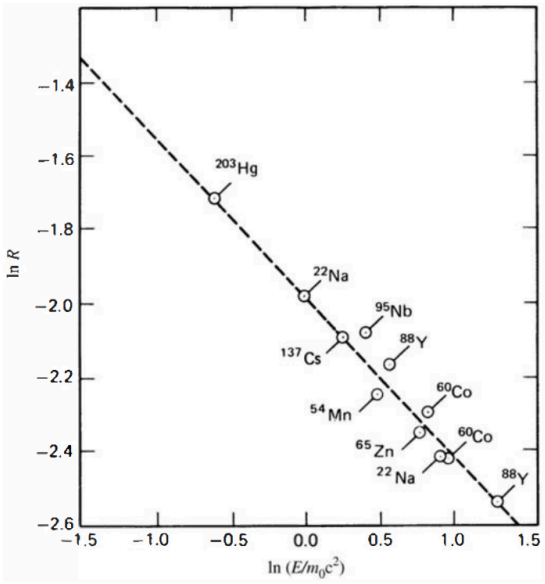

Figure 11: Measured $\ln R$ vs $\ln E$ from a NaI(Tl) detector

There are still other factors that affect the energy resolution, which include:

- variations in light generation and measurement
- non proportionality of light yield
- long term drift

4.3. Engergy Calibration

Perfect proportionality between light output and deposited energy in scintillators would yield a linear calibration of pulse height or centroid channel number for full-energy peaks vs gamma-ray energy.

However, due to inherent nonproportionality in scintillator responses to fast electrons, calibrations typically exhibit some nonlinearity, resulting in curved peak positions specific to each detector.

But normally the assumption of linearity leads to negligible error.

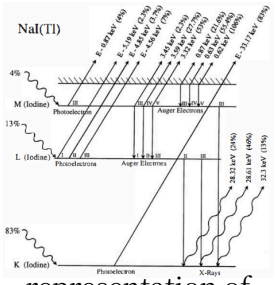

representation of the possible origins of electrons and photons[3]

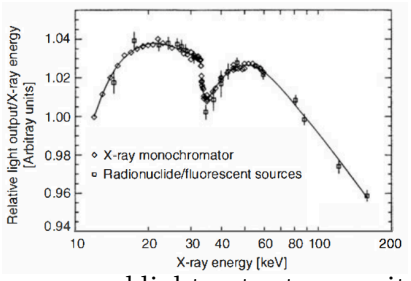

measured light output per unit deposited energy for Nal (Tl), normalized to unity at 88 keV

Figure 12: Complex energy origin and non linearity response

The measured relative light output from sodium iodide over the low energy range is presented in Figure 12. There is a dip near the K-shell absorption edge of iodine. The response of the scintillator actually depends on the energy that is deposited by secondary electrons produced by the incident photon, and a complex mix of photoelectrons and/or Auger electrons will result from various types of photon interactions.

4.4. Detection Efficiency

Common application of sodium iodide scintillators is to measure the absolute intensity, which requires a prior knowledge of the effeiency of radiation detector. And published data on the detection efficiency of NaI(Tl) detectors are undoubtedly abundant.

[3] following the photoelectric absorption of an incident X-ray or gamma ray with energy E that is above the K-shell binding energy of 33.17 keV

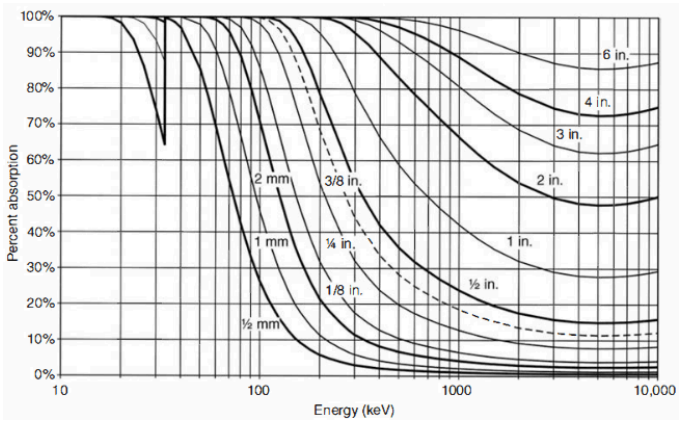

Figure 13: Absorption efficiency of NaI of different thicknesses

,

Appendix

Periodic Table

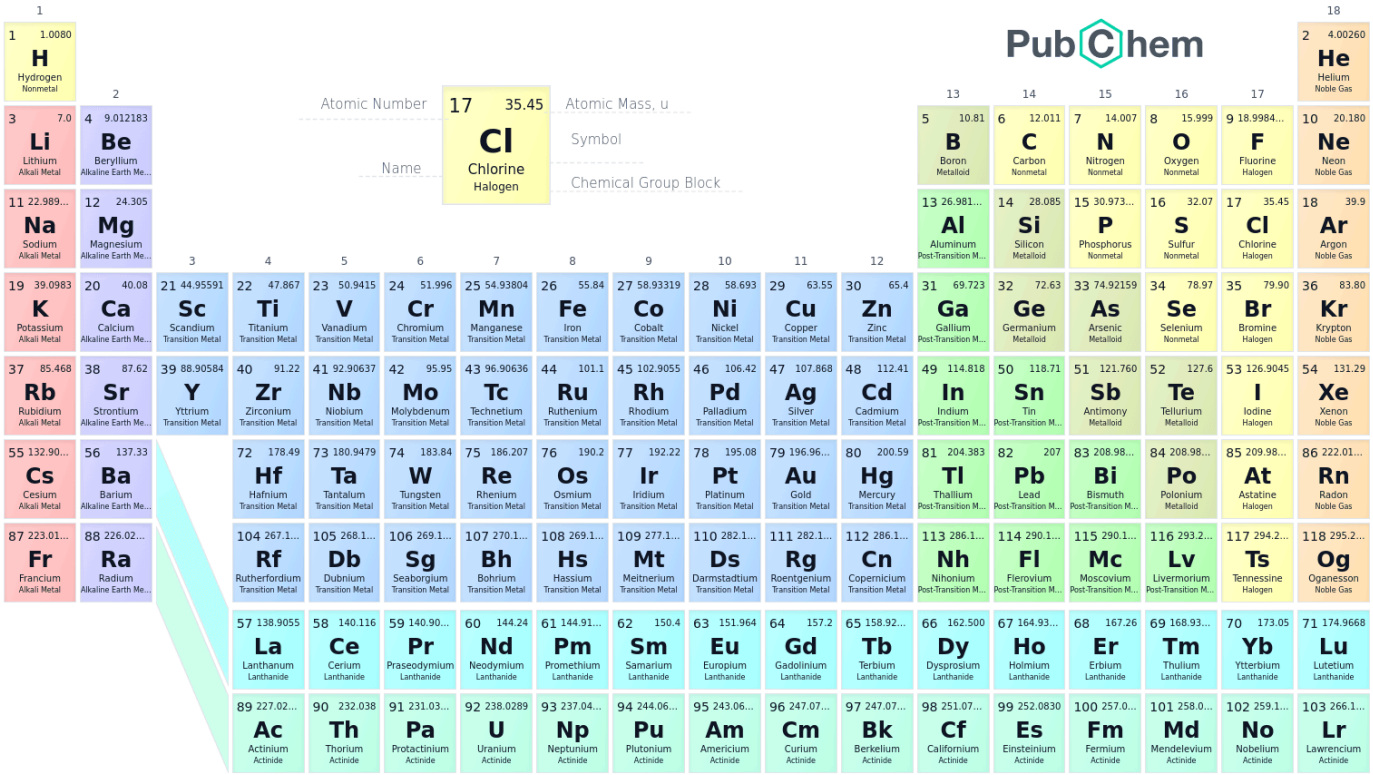

Figure 14: Periodic Table

,

Terminologies

I refered to 電機工程學術名詞 for the translation of some terms.

ABBR.	Term	术语
	attenuation	衰减
	deposit	沉积
STP	standard temperature and pressure	标准状况
	recoil	反冲
	photopeak	光电峰
	photofraction	峰总比
	encapsulation	封装
	graded shield	梯度屏蔽
	true coincidence	真符合
	chance coincidence	偶然符合
	sum peak	和峰
BGO	bismuth germanate oxide	锗酸铋
	scintillation efficiency	闪烁效率

Table 1: Terminologies